



Contents lists available at ScienceDirect

# Journal of Computational and Applied Mathematics

journal homepage: [www.elsevier.com/locate/cam](http://www.elsevier.com/locate/cam)

## Shape and topology optimization of an acoustic horn–lens combination

Eddie Wadbro<sup>a,\*</sup>, Rajitha Udawalpola<sup>a</sup>, Martin Berggren<sup>b</sup><sup>a</sup> Division of Scientific Computing, Department of Information Technology, Uppsala University, Box 337, SE-751 05 Uppsala, Sweden<sup>b</sup> Department of Computing Science, Umeå University, SE-901 87 Umeå, Sweden

### ARTICLE INFO

#### Article history:

Received 30 November 2007

Received in revised form 30 May 2008

#### Keywords:

Design optimization

Helmholtz equation

Acoustic horn

Acoustic lens

### ABSTRACT

Using gradient-based optimization combined with numerical solutions of the Helmholtz equation, we design an acoustic device with high transmission efficiency and even directivity throughout a two-octave-wide frequency range. The device consists of a horn, whose flare is subject to boundary shape optimization, together with an area in front of the horn, where solid material arbitrarily can be distributed using topology optimization techniques, effectively creating an acoustic lens.

© 2009 Elsevier B.V. All rights reserved.

## 1. Introduction

We study acoustic devices operating as part of a loudspeaker system for use in large auditoriums or outdoors. Horns are used in such systems to enhance the efficiency of the sound generation as well as to direct the sound toward the audience. Thus, two main characteristics of an acoustic horn are its transmission efficiency and directivity properties. For large arena events, sound energy should not be wasted at directions of no audience. Moreover, each member of the audience should ideally be exposed to the same sound quality, that is, the efficiency and directivity properties of a horn need to be as uniform as possible throughout the operating frequency range. Bångtsson et al. [1] attacked the problem of designing an efficient horn using boundary shape optimization of the horn flare. Admissible flare shapes were given by functions  $\beta$ , prescribing the normal deflection from a straight horn (Fig. 1). Wadbro and Berggren [2,3] instead applied topology optimization, allowing an arbitrary material distribution in the interior of the horn, to design an efficient horn with requirements on the directivity. Recently, Udawalpola and Berggren [4] performed boundary shape optimization to study the tradeoff between efficiency and directivity requirements. Their results suggest that manipulations of the horn flare are sufficient to design highly efficient devices. However, these horns exhibit a marked beaming effect, that is, the directional pattern narrows as the frequency increases. Breaking the beaming behavior using only modifications of the flare shape comes with a substantial penalty on efficiency, at least when restricting attention to planar or cylindrical symmetry. Here, we use shape and topology optimization simultaneously to design an efficient horn–lens combination with even directivity for a wide range of frequencies.

## 2. Problem statement

The setup used as a basis for optimization, illustrated in Fig. 1, is inspired by the classical horn–lens combinations conceived by Kock and Harvey [5] in the 1940s. The geometry is assumed to be infinite in the direction normal to the plane.

\* Corresponding author. Tel.: +46 18 471 2965; fax: +46 18 52 3049.

E-mail addresses: [eddie.wadbro@cs.umu.se](mailto:eddie.wadbro@cs.umu.se) (E. Wadbro), [rajitha.udawalpola@it.uu.se](mailto:rajitha.udawalpola@it.uu.se) (R. Udawalpola), [martin.berggren@cs.umu.se](mailto:martin.berggren@cs.umu.se) (M. Berggren).

<sup>1</sup> Present address: Department of Computing Science, Umeå University, SE-901 87 Umeå, Sweden.

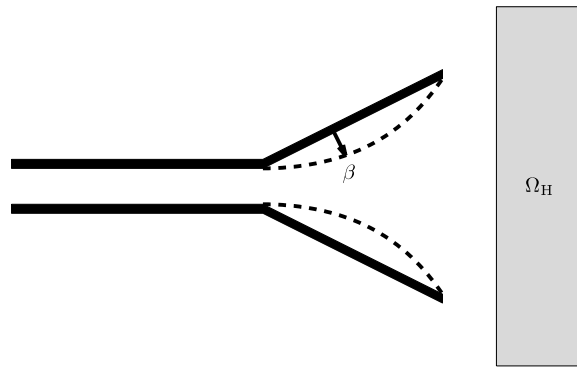


Fig. 1. The walls of the horn are displaced and material is placed in the region  $\Omega_H$  to improve the radiation properties.

The device consists of a waveguide with a conical termination (the horn) and a lens located in front of the horn. The width of the waveguide (the throat of the horn) is 10 cm, the length of the horn is 50 cm, and the width of the mouth is 60 cm. The lens area is located 15 cm in front of the horn and is 25 cm deep and 100 cm wide. The 2D setup may be viewed as a simplified model of a wide rectangular horn. Such horns are used to achieve a wider horizontal than vertical sound distribution.

To study the characteristics of the device, we impose a right-going planar wave with amplitude  $A$  and frequency  $\omega$  in the waveguide. The horn and the lens will guide the transmission of the wave into free space, but parts of the wave will also be reflected back into the waveguide. The device is said to be efficient if a large portion of the incoming wave energy is transmitted into free space. The directivity describes the far-field distribution of the transmitted wave energy. The efficiency and the directivity of the device are dependent on its design as well as the frequency of the transmitted wave. We are interested in designing an efficient horn that spreads the sound energy uniformly and frequency independently within a given angle around the horn axis.

We assume that the wave propagation is governed by the linear wave equation for fluctuations  $P'$  in the acoustical pressure. We seek time harmonic solutions for a single angular frequency  $\omega$  using the ansatz  $P'(x, t) = \Re\{p(x)e^{i\omega t}\}$  and find that the complex amplitude function  $p$  satisfies the Helmholtz equation

$$\Delta p + k^2 p = 0, \tag{1}$$

where  $k = \omega/c$  is the wavenumber and  $c$  the speed of sound. We assume that the waveguide and the horn consist of sound hard material. Further, we stipulate that  $p$  satisfies the Sommerfeld radiation condition, which specifies that all waves are outgoing in the far field.

Wave propagation in the waveguide can be expressed as a superposition of modal components satisfying the Helmholtz equation (1) together with the boundary condition

$$\frac{\partial p}{\partial n} = 0 \tag{2}$$

along the sound hard walls. If the width of the waveguide is sufficiently small compared to the wavelength, the non-planar modes are geometrically evanescent. The left boundary of the truncated waveguide is denoted  $\Gamma_{in}$ . The boundary condition

$$i\omega p + c \frac{\partial p}{\partial n} = 2i\omega A \quad \text{on } \Gamma_{in} \tag{3}$$

imposes a right-going wave with amplitude  $A$  and absorbs left-going waves. The boundary condition (2) is used for the boundaries corresponding to the sound hard walls of the horn as well as for the symmetry boundary  $\Gamma_{sym}$ . We solve wave propagation problem (1) numerically using the finite element method. The unbounded domain is truncated to a rectangular domain using a perfectly matched layer (PML), marked gray in Fig. 2, to handle the outgoing wave property. Following Heikkola et al. [6], we define

$$\gamma_k = 1 - i\sigma_0 \frac{\sigma_k}{\omega}, \quad k = 1, 2, \quad \gamma = \gamma_1 \gamma_2, \quad D = \begin{pmatrix} \gamma_2/\gamma_1 & 0 \\ 0 & \gamma_1/\gamma_2 \end{pmatrix},$$

where  $\sigma_0$  is a non-negative constant,

$$\sigma_1 = \max(0, \max(x_1 - \bar{x}_1 + \delta, x_1 + \delta - x_1)), \quad \sigma_2 = \max(0, x_2 - \bar{x}_2 + \delta),$$

and where  $\bar{x}_1$  and  $\bar{x}_2$  are the coordinates for the left and right edge of the computational domain  $\Omega$ , depicted in Fig. 2, respectively. Similarly,  $\bar{x}_2$  corresponds to upper edge, and  $\delta$  is the width of the PML layer. We modify (1) to include the PML as follows:

$$\nabla \cdot (D\nabla p) + k^2 \gamma p = 0 \quad \text{in } \Omega. \tag{4}$$

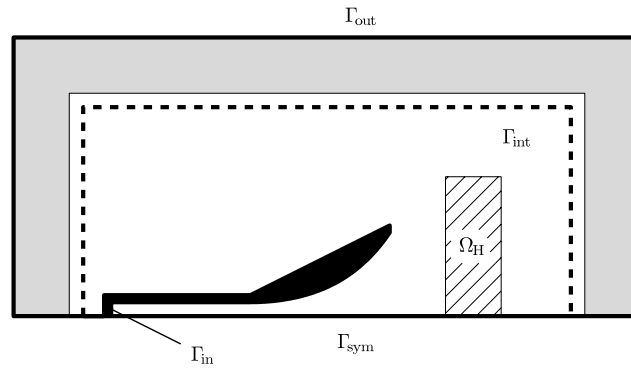


Fig. 2. The computational domain  $\Omega$ .

Petropoulos [7] reports that the boundary condition terminating the PML does not have a significant effect on accuracy when the loss profile is linear or quadratic. In our experiments, we use boundary condition (2) at the outer boundary  $\Gamma_{out}$ .

We optimize the horn–lens combination presented in Fig. 1, allowing the horn flare to deflect normal to the funnel shaped reference flare and allowing sound hard material to fill an arbitrary region  $\Omega_m$  within  $\Omega_H$  ( $\Omega_H - \Omega_m$  consists of air). The function  $\beta$  denotes the perpendicular displacement of the horn flare from the reference funnel shape, and  $\Omega^\beta$  denotes the computational domain with the flare shape specified by  $\beta$ . Since the Neumann boundary condition (2) holds on  $\partial\Omega_m$  and can be imposed as a “natural” boundary condition by simply removing the  $\Omega_m$  region from the integrals, the variational form of the wave propagation problem for a single frequency can be written as follows:

Find  $p \in H^1(\Omega^\beta - \Omega_m)$  such that

$$\int_{\Omega^\beta - \Omega_m} \nabla q \cdot (D\nabla p) - k^2 \int_{\Omega^\beta - \Omega_m} \gamma q p + ik \int_{\Gamma_{in}} q p = 2ikA \int_{\Gamma_{in}} q, \quad \forall q \in H^1(\Omega^\beta - \Omega_m). \tag{5}$$

We parameterize the region  $\Omega_m$  using a material indicator function  $\alpha : \mathbb{R}^2 \rightarrow \{0, 1\}$  defined such that  $\alpha(x) = 0$  if  $x$  is at a point in the solid material and  $\alpha(x) = 1$  if  $x$  is at a point in air. Thus,  $\Omega_m = \{x \in \Omega^\beta \mid \alpha(x) = 0\}$ , and we utilize this definition to replace equation (5) with the following variational form:

Find  $p \in H^1(\Omega^\beta)$  such that

$$\int_{\Omega^\beta} \alpha \nabla q \cdot (D\nabla p) - k^2 \int_{\Omega^\beta} \alpha \gamma q p + ik \int_{\Gamma_{in}} q p = 2ikA \int_{\Gamma_{in}} q, \quad \forall q \in H^1(\Omega^\beta). \tag{6}$$

In order to obtain a unique solution of problem (6) (also inside  $\Omega_m$ ), we redefine  $\alpha$  such that  $\alpha(x) \in \{\varepsilon, 1\}$  for all  $x \in \Omega_H$ , where  $\varepsilon$  is a small positive number.

The transmission efficiency of the device for a certain frequency  $\omega$  can be measured by observing the mean complex amplitude  $\langle p \rangle_{in}$  on  $\Gamma_{in}$ . The mean complex amplitude of the reflected left-going wave at  $\Gamma_{in}$  is given by  $\langle p \rangle_{in} - A$ . The horn is efficient if the magnitude  $|\langle p \rangle_{in} - A|$  of the reflected wave is small compared to the magnitude  $|A|$  of the incoming wave.

In the far field, the complex amplitude function is essentially the product of a function of the distance to the device and a function of the direction. More precisely, let  $p$  be the solution to the exterior Helmholtz problem (1) satisfying the Sommerfeld radiation condition in the far-field, boundary condition (3) at the inlet, and (2) along the sound hard walls. Let  $\hat{x}(\theta)$  be a point on the unit sphere, where  $\theta$  denotes the polar argument of  $\hat{x}$ ; then

$$p(\hat{x}(\theta)\rho) = \frac{e^{ik\rho}}{\sqrt{\rho}} \left\{ p_\infty(\theta) + O\left(\frac{1}{\rho}\right) \right\} \quad \text{as } \rho \rightarrow \infty,$$

where  $\rho$  represents the distance from the device. The function  $p_\infty(\theta)$  is called the far-field pattern. An expression for  $p_\infty(\theta)$  can be derived using classical methods from scattering theory (Colton & Kress [8]), and is for planar symmetry given by

$$p_\infty(\theta) = \frac{1-i}{4\sqrt{\pi k}} \int_\Gamma e^{ik\hat{x} \cdot x} \left( ip(x)k\hat{x} \cdot n(x) - \frac{\partial p}{\partial n}(x) \right) d\mathcal{H}^1(x), \tag{7}$$

where  $\Gamma$  is any closed curve that forms the boundary of a domain containing all sound sources (the device) and  $n(x)$  the outward directed normal at  $x \in \Gamma$ . Here, we substitute the solution of the truncated problem (6) and the dashed interior boundary  $\Gamma_{int}$  into expression (7) in order to compute a numerical approximation of the far-field pattern, as detailed in [9].

We are interested in designing an efficient device with an even directivity pattern for a wide frequency band. We minimize the magnitude of the reflected waves throughout the considered frequency band to obtain an efficient device. To achieve an even acoustical pressure distribution within a given angle in front of the device, we minimize the difference in magnitude in the far-field pattern between the horn axis and at angles equispaced centered at the horn axis. Moreover,

to avoid designs that give an even pressure distribution in front of the horn at the price of scattering the transmitted wave in other directions (backscattering), we minimize the far-field pressure at selected angles, such as behind and at the sides of the device.

The above requirements on efficiency, backscattering, and directivity comprise the terms in the objective function

$$J(\alpha, \beta) = \sum_{\omega_j} \left( \left| p^{(\omega_j)}_{\text{in}} - A \right|^2 + \sigma_b \sum_{\vartheta_k} \left| p_{\infty}^{(\omega_j)}(\vartheta_k) \right|^2 + \sigma_f \sum_{\theta_l} \left| \left| p_{\infty}^{(\omega_j)}(\theta_l) \right|^2 - \left| p_{\infty}^{(\omega_j)}(\theta_0) \right|^2 \right|^2 \right), \quad (8)$$

where  $\omega_j$  are the frequencies for which we optimize the device,  $\theta_l$  are the angles where we aim for even radiation ( $\theta_0$  is the reference angle which corresponds to the horn axis), and the angles  $\vartheta_k$  are introduced to minimize the backscattering. The constants  $\sigma_b$  and  $\sigma_f$  set the relative weights of the different objectives.

To complete the formulation of the optimization problem, we need to specify the admissible designs for  $\alpha$  and  $\beta$ . Following Bångtsson et al. [1], the perpendicular distance  $\beta$  from the reference shape is indirectly represented as the solution to the differential equation  $-\beta'' = \eta$ , with  $\beta = 0$  at the throat and mouth of the horn. In order to promote smooth design updates of horn flare, we use  $\eta$ , which roughly corresponds to the curvature of the horn flare, as design variable.

For the optimization of the lens, we want to find the optimal binary-valued material distribution function  $\alpha$ . Such optimization problems are often severely ill-posed in the sense that they lack solutions: there exists minimizing sequences of material distribution functions that contains no subsequence that converges in any reasonable way. Such ill-posedness typically manifests itself in the discrete case as a mesh dependency of the optimal designs; that is, the optimal design may drastically change when the mesh is refined, as finer and finer details occur. Another difficulty is that the discretized problem constitutes a large-scale nonlinear integer programming problem that is difficult to handle numerically. To handle the latter problem, we follow a well established strategy developed for problems in linear elasticity [10], a strategy that in the end also will cure the first problem. The strategy operates in three steps: *relaxation*, *penalty*, and *filtering*.

In the first step, we relax the space of admissible designs to the continuum  $\alpha \in [\varepsilon, 1]$  in order to allow the use of a gradient-based optimization algorithm. In general, such a relaxation can be expected to destroy the binary nature of the problem. At the same time, the relaxation may regularize the problem and generate mesh independent, albeit non-binary (“gray”) designs in the discrete case. However, as the mesh dependent designs in Fig. 4 illustrate, the relaxation seems not to regularize the problem in this case.

The next step, penalty, addresses the problem of non-binary optimal designs in the relaxed problem, and introduces a penalty term, for instance the one we use,

$$J_p = \int_{\Omega_H} (\alpha - \varepsilon)(1 - \alpha),$$

in the objective function (or as a constraint) to promote values close to  $\varepsilon$  or 1. Unfortunately, the addition of such a term aggravates the ill-posedness of the optimization problem.

An issue related to the ill-posedness problem is the lack of control over the size of the structural parts. It is practical to be able to specify a parameter  $\tau > 0$  to impose a lower bound on the extension of individual structural parts independently of the mesh size. In the third step of our strategy, we therefore introduce a new design variable  $\tilde{\alpha}$  and define  $\alpha$  indirectly through the convolution  $\alpha = K_{\tau} * \tilde{\alpha}$ , where  $K_{\tau}$  is an integral operator kernel with support in a neighborhood of radius  $\tau$  that provides a local averaging of the design variable. This procedure, known as *filtering* in the topology optimization community, helps to enforce mesh independent solutions and also combats purely numerical artifacts such as checkerboarding [11]. Bourdin [12] studies a filtered and penalized version of the minimum compliance beam design problem, proves existence of solutions, and shows convergence of solutions to the finite element discretized version of this problem. Although we know of no analogous proof for the Helmholtz equation (the proof would be substantially more difficult because of the non-coerciveness of the variational problem), all our numerical experience, both the one reported earlier [2] and the one presented below, indicates that the filtering strategy affects the optimal designs in an analogous way to the compliance minimization problem. That is, the numerical instabilities disappear and the results suggest mesh convergence in the limit of refinements.

We thus state our general optimization problem as

$$\min_{\tilde{\alpha}, \eta} \left[ \sigma_{\eta} \int_{\Gamma_{\text{ref}}} \eta^2 + \sigma_{\alpha} \int_{\Omega_H} (K_{\tau} * \tilde{\alpha} - \varepsilon)(1 - K_{\tau} * \tilde{\alpha}) + J(K_{\tau} * \tilde{\alpha}, \beta(\eta)) \right], \quad (9)$$

where the first term is a Tichonov regularization term for the horn flare and the second term provides penalty and filtering. The constants  $\sigma_{\eta}$  and  $\sigma_{\alpha}$  are used specify the amount of regularization and penalty, respectively. For further details about the discretization, handling of mesh deformations, and the sensitivity analysis with respect to the different terms in the objective function, we refer to our earlier works [1,2,4].

### 3. Numerical experiments

We solve optimization problem (9) numerically using the Method of Moving Asymptotes (MMA) [13]. MMA is a gradient-based optimization method that is particularly well suited for the mathematical structure of topology optimization

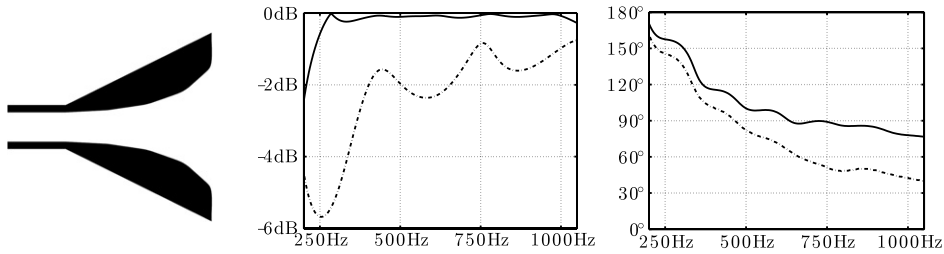


**Fig. 3.** Horn without lens optimized for high efficiency and even directivity using only modifications of the horn flare (left), the transmission loss in dB (middle), and the beamwidth (right) as functions of frequency. The dash-dotted lines in the diagrams illustrate efficiency and directivity properties for our funnel shaped reference horn.

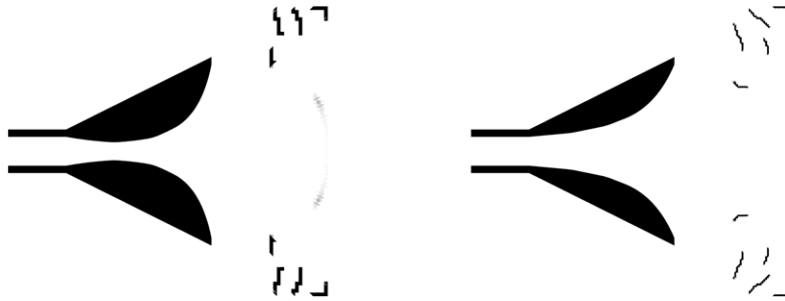


**Fig. 4.** Horn–lens combinations optimized for high efficiency and even directivity using modifications of the horn flare and allowing the material function in  $\Omega_H$  attain values in the continuum  $[\varepsilon, 1]$ . Both devices are optimized on the same mesh. Left: using a coarse material representation (1600 unknowns), right using the regular material representation (6400 unknowns).

problems. Note that we optimize simultaneously for the horn flare and the lens area. We aim to design a device with high efficiency as well as even directivity throughout a wide frequency range. In this section, we illustrate the performance of the optimized devices with two diagrams: the *transmission loss* and the *beamwidth* of the device. The transmission loss is the relative loss with respect to a perfect transmission of the incoming wave. Here we illustrate the transmission loss as

$$T = 20 \log_{10} \left( 1 - \frac{|B|}{|A|} \right),$$

where  $A$  and  $B$  are the amplitudes of the right- and left-going waves in the waveguide respectively. The beamwidth of the device is defined as the angle between the  $-6$  dB points closest to the horn axis of the relative directional intensity

$$d(\theta) = 20 \log_{10} \left( \frac{|p_\infty(\theta)|}{\max_\varphi |p_\infty(\varphi)|} \right).$$

In our experiments, we aim for a high efficiency and a  $100^\circ$  beamwidth in the two-octave-wide frequency range 250–1000 Hz. We therefore optimize the device for even directivity at the angles  $0^\circ, \pm 10^\circ, \dots, \pm 50^\circ$  with respect to the horn axis for frequencies exponentially spaced with 12 frequencies per octave. The angles  $90^\circ$  and  $180^\circ$  are used to minimize the back scattering. That is, we set the frequencies and angles in objective function (8) as follows:  $\omega_k = 250 \cdot 2^{k/12}$ ,  $k = 0, 1, \dots, 24$ ,  $\theta_l = l \cdot 10^\circ$ ,  $l = 0, 1, \dots, 5$ ,  $\vartheta_0 = 180^\circ$ , and  $\vartheta_1 = 90^\circ$ . In our experiments, we set the relative weights for the different objectives as:  $\sigma_b = \sigma_f = \frac{1}{2}$ , and set  $\sigma_\eta = 10^{-5}$ . We set  $\varepsilon = 10^{-3}$  and use a continuation approach for the penalization. That is, we first solve the problem without penalty ( $\sigma_\alpha = 0$ ), then the problem is solved again using  $\sigma_\alpha = 10^{-5}$  with the unpenalized solution as starting guess. The process is then repeated using  $\sigma_\alpha = 10^{-4}, 10^{-3}, \dots, 10$  and the previous solution as starting guess.

In our first experiment, we attempt to design an optimal device using only modifications of the horn flare. Fig. 3 shows the resulting optimized device together with diagrams illustrating its transmission loss and beamwidth as functions of frequency (solid lines). These diagrams also illustrate the behavior of our funnel shaped reference horn (dash-dotted lines). The optimized horn is superior to the reference horn both with respect to efficiency and directivity throughout the frequency band of study. The optimized horn exhibits a maximum transmission loss of 0.6 dB as shown in the top right diagram. The beamwidth for the both horns demonstrates a decreasing trend throughout the frequency range and is less than  $80^\circ$  at 1000 Hz for the optimized horn and about  $45^\circ$  at 1000 Hz for the reference shape.

Our plan to break this narrowing of the beamwidth is to place material in front of the horn using topology optimization. As an initial test, we perform optimization without penalty ( $\sigma_\alpha \equiv 0$ ) and without filtering ( $K_\tau * \alpha \equiv \alpha$ ). Fig. 4 illustrates two devices optimized without penalty or filter. The optimized devices are very efficient and exhibit a large beamwidth

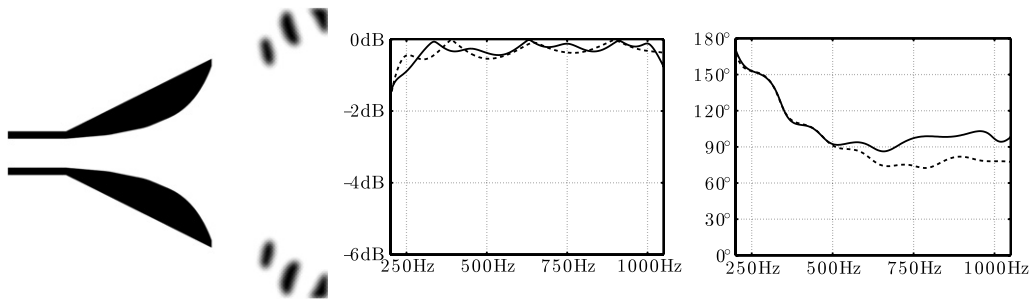


**Fig. 5.** Horn with lens optimized for high efficiency and even directivity using modifications of the horn flare and topology optimization (with penalty and filter) of the lens in front of the horn (left), the transmission loss in dB (middle), and the beamwidth (right) as functions of frequency. The solid lines in the diagrams correspond to the horn–lens combination, while the dashed line illustrates the performance of this horn without the lens.

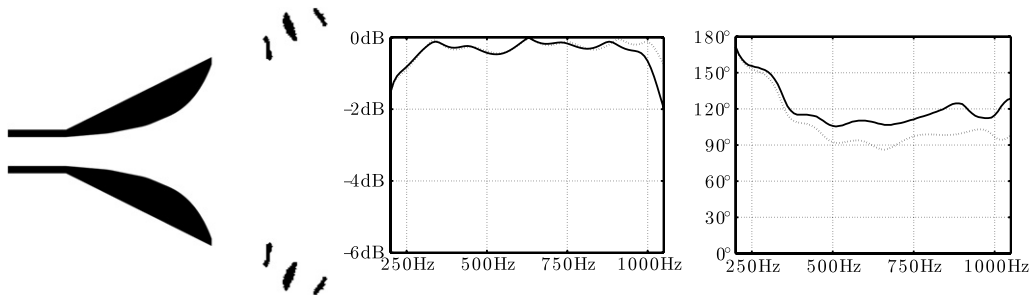


**Fig. 6.** Postprocessed version of the horn–lens combination in Fig. 5, obtained using unfiltered topology optimization to sharpen the lens portion of the device (left), the transmission loss in dB (middle), and the beamwidth (right) as functions of frequency. The dotted lines correspond to the initial (unpostprocessed) horn–lens combination depicted in Fig. 5.

throughout the frequency range. Both these devices are computed using the same mesh, but with different representations for the material indicator function, with 1600 and 6400 unknown densities. The device to the right is computed with  $\alpha$  constant on each element of the finite element mesh, whereas  $\alpha$  for the left device is constant on groups of four adjacent elements (constructed as a regular unrefinement of the mesh in the lens region). The resulting designs in the lens region are mesh dependent and contain one-material-element-wide structures, suggesting thin sheets of sound hard material; but regions of intermediate densities also appear. For other choices of angles, frequencies, and weights in the objective function, these intermediate density regions are more pronounced than those appearing in the lens on the left device in Fig. 4.

The device in Fig. 5 is designed simultaneously using shape optimization of the horn flare and topology optimization for the lens in front of the horn. A continuation approach as described above is used for the penalization, and a filter with radius  $\tau = 2.5$  cm is employed. The grayness at solid boundaries in the lens area is an unavoidable consequence of the use of filters. Our experiments suggest that the present setup, using a continuum approach for the penalization together with a filtering procedure, produces mesh independent designs of the horn flare and the lens. The dashed lines in the diagrams illustrate the performance of this horn without the lens. The influence of the lens can be seen by comparing the dashed and the solid lines in the diagrams. Both devices (horn with lens and horn without lens) are very efficient throughout the frequency range subject to the optimization, with maximum transmission losses of 0.6 dB and 0.9 dB for the horn without and with lens, respectively, as shown in the middle diagram of Fig. 5. Comparing the beamwidths (right diagram) of these devices, it can be seen that the lens has a large influence on the far-field behavior for the higher frequencies, but only a minor influence at the lower frequencies. The beamwidth of the device optimized with lens is well controlled and stays above  $90^\circ$ , except for a small frequency band around 650 Hz. In essence, the addition of a lens only has a minor influence on the transmission efficiency, while it successfully breaks the beaming behavior of the horn.

Fig. 6 shows a postprocessed version of the lens design in Fig. 5, after applying a procedure that removes the gray while attending the design objective [2]. The postprocessing consists of an optimization round using the setup in Fig. 5 as a starting guess, keeping the horn flare fixed, and applying topology optimization with penalty but without filtering to sharpen the boundary of the lens. The solid lines in the diagrams in Fig. 6 are computed on a body-fitted mesh for the postprocessed device, while the dotted lines, corresponding to the unpostprocessed device, are computed using the material modeling of Eq. (6). The sharpening of the lens structure only has a minor influence on the efficiency of the device. The efficiency of the devices is almost identical for frequencies up to 900 Hz. For frequencies near the upper edge of the frequency band, the postprocessed device is slightly less efficient. There is, however, a marked difference in the far-field behavior between the postprocessed and the unpostprocessed device. The postprocessing sharpens the contrast between the air and the solid material for the objects comprising the lens. In the unpostprocessed case, these solid objects are surrounded by gray material, functioning as a smooth transition between the air and the solid. The harder edges of the postprocessed device enables more

direct control of the far-field behavior and the postprocessed device manages to keep the beamwidth above  $105^\circ$  throughout the two-octave-wide frequency range.

#### 4. Conclusions

Combining shape and topology optimization, we manage to design efficient acoustic horn–lens combinations that break the beaming behavior for higher frequencies. The strategy we use to optimize the material distribution in the lens region (relaxation, penalization, filtering, and postprocessing) successfully produces mesh independent designs with prescribed performance within a given angle and frequency range.

#### Acknowledgment

Funding for the research was provided by the Swedish Research Council and Swedish International Development Cooperation Agency (SIDA).

#### References

- [1] E. Bångtsson, D. Noreland, M. Berggren, Shape optimization of an acoustic horn, *Computer Methods in Applied Mechanics and Engineering* 192 (2003) 1533–1571.
- [2] E. Wadbro, M. Berggren, Topology optimization of an acoustic horn, *Computer Methods in Applied Mechanics and Engineering* 196 (2006) 420–436.
- [3] E. Wadbro, M. Berggren, Topology optimization of wave transducers, in: M.P. Bendsøe, N. Olhoff, O. Sigmund (Eds.), *IUTAM Symposium on Topological Design Optimization of Structures, Machines and Materials*, Springer, 2006, pp. 301–310.
- [4] R. Udawalpola, M. Berggren, Optimization of an acoustic horn with respect to efficiency and directivity, *International Journal for Numerical Methods in Engineering* 73 (11) (2008) 1571–1606.
- [5] W.E. Kock, F. Harvey, Refracting sound waves, *The Journal of the Acoustical Society of America* 21 (5) (1949) 471–481.
- [6] E. Heikkola, T. Rossi, J. Roivanen, Fast direct solution of the Helmholtz equation with a perfectly matched layer or an absorbing boundary condition, *International Journal for Numerical Methods in Engineering* 57 (14) (2003) 2007–2025.
- [7] P.G. Petropoulos, On the termination of the perfectly matched layer with local absorbing boundary conditions, *Journal of Computational Physics* 143 (2) (1998) 665–673.
- [8] D. Colton, R. Kress, *Integral Equation Methods in Scattering Theory*, John Wiley & Sons Inc., 1983.
- [9] E. Wadbro, On the far-field properties of an acoustic horn, Tech. Rep. 2006-042, Department of Information Technology, Uppsala University, 2006.
- [10] M.P. Bendsøe, O. Sigmund, *Topology Optimization. Theory, Methods, and Applications*, Springer, 2003.
- [11] T. Borrvall, Topology optimization of elastic continua using restriction, *Archives of Computational Methods in Engineering* 8 (4) (2001) 351–385.
- [12] B. Bourdin, Filters in topology optimization, *International Journal for Numerical Methods in Engineering* 50 (2001) 2143–2158.
- [13] K. Svanberg, The method of moving asymptotes—a new method for structural optimization, *International Journal for Numerical Methods in Engineering* 24 (1987) 359–373.